NBS1 binds directly to TOPBP1 via disparate interactions between the NBS1 BRCT1 domain and the TOPBP1 BRCT1 and BRCT2 domains

Oanh Huynh[1], Kenna Ruis[1], Katrina Montales[1], and W. Matthew Michael[1,2]

[1]Molecular and Computational Biology Section

Department of Biological Sciences

University of Southern California

Los Angeles, CA 90089

[2]Author for correspondence at: mattm@usc.edu

Abstract

The TOPBP1 and NBS1 proteins are key components of DNA repair and DNA-based signaling systems. TOPBP1 is a multi-BRCT domain containing protein that plays important roles in checkpoint signaling, DNA replication, and DNA repair. Likewise, NBS1, which is a component of the MRE11-RAD50-NBS1 (MRN) complex, functions in both checkpoint signaling and DNA repair. NBS1 also contains BRCT domains, and previous works have shown that TOPBP1 and NBS1 interact with one another. This interaction occurs efficiently under basal conditions and efficiency increases during a DNA damage response (DDR). In this work we examine the basal interaction between TOPBP1 and NBS1, and we show that the two proteins bind to one another in a non-canonical manner. We report that NBS1 uses its BRCT1 domain to directly interact with a central region of TOPBP1's BRCT1, and that it also binds to a C-terminal region within TOPBP1's BRCT2 domain. Thus, NBS1 can interact with TOPBP1 via two different modes of binding. For both of TOPBP1's BRCT1 and BRCT2 domains we delineate short peptide sequences, less than 30 amino acids, that are sufficient for binding to NBS1 and can confer binding upon transfer to a heterologous protein, such as maltose binding protein (MBP). We also show that NBS1 requires an intact phosphate-binding pocket (PBP) within its BRCT1 domain to interact with TOPBP1, however the presence of phosphate is not required for binding. These data expand our understanding of how BRCT-containing proteins bind to one another by revealing a non-canonical mode of binding and by showing that PBPs can contribute to binding in a phosphate-independent manner.

35 **Key words**

36 BRCT domain, TOPBP1, NBS1, MRN complex, protein-protein interaction, scaffold

37 protein

38 **1. Introduction**

39 Scaffold proteins are platforms for the assembly of multi-protein complexes
40 and are key contributors to the cellular response to DNA damage. Scaffolds typically
41 contain multiple domains that allow for either protein::protein or protein::nucleic
42 acid interactions, and they function by recruiting multiple partners and bringing
43 these disparate factors together in a manner that nucleates DNA-based signaling
44 and repair complexes (Reinhardt and Yaffee, 2013; Wan et al, 2016; Day et al, 2021).
45 One well-studied scaffold is the XRCC1 protein, an excision repair factor that binds
46 to damaged chromatin via interaction with auto-modified PARP1, and in turn
47 recruits DNA polymerase beta and DNA ligase III to facilitate repair of the lesion.
48 The modular structure of XRCC1 explains its function as XRCC1 uses three distinct
49 domains to bind damaged chromatin, bind DNA polymerase beta, and to bind DNA
50 ligase III (London, 2020). Another well-studied scaffold protein is TOPBP1, which
51 plays numerous roles in the cell including checkpoint signaling, DNA repair, DNA
52 replication, and transcription (Day et al, 2021; Bagge et al, 2021; Ma et al, 2020;
53 Wardlaw et al, 2013). TOPBP1's scaffold function has been most clearly
54 demonstrated in yeast during the initiation of DNA replication, where the TOPBP1
55 ortholog DPB11 binds both SLD3 and SLD2 to allow activation of the replicative
56 helicase (Costa and Diffley, 2022). TOPBP1 may also play a scaffolding role during
57 DNA damage signaling. Using a cytological assay, recent work has suggested that
58 TOPBP1 physically links the DNA signaling proteins 53BP1 and RAD9 together at
59 sites of damage in G1 cells (Bigot et al, 2019). Other work has also promoted a
60 scaffold function for TOPBP1, during RAD51 filament formation for DNA double-

61 strand break (DSB) repair. In this scenario, TOPBP1 binds both PLK kinase and
62 RAD51, thereby promoting RAD51 phosphorylation by PLK, a step required for
63 filament formation (Moudry et al, 2016).
64
65 For scaffolds to function they must contain sequence motifs that allow for
66 interaction with exogenous binding partners. One such motif that is prominent
67 amongst proteins involved in the DDR is the BRCA1 C-Terminal repeat, or BRCT
68 domain. BRCT domains are multi-faceted protein-protein interaction domains that
69 also have the capacity to bind DNA (Sheng et al, 2011), as well as the poly ADP
70 ribose (PAR) chains synthesized by PARP enzymes at sites of damage (Hou et al,
71 2019). One well-studied feature of BRCT domains is their ability to bind substrate
72 proteins in a manner regulated by substrate phosphorylation (Leung and Glover,
73 2011; Reinhardt and Yaffee, 2013; Day et al, 2021). A subset of BRCT domains
74 contain so-called phosphate-binding pockets (PBPs), whereby a triad of highly
75 conserved residues within the BRCT domain come together to form a phosphate-
76 binding surface that promotes interaction with phosphorylated substrates (Leung
77 and Glover, 2011; Reinhardt and Yaffee, 2013; Day et al, 2021). Another feature that
78 can distinguish different classes of BRCT domains is whether they appear as a single
79 module, or two or even three closely spaced modules (Sheng et al, 2011).
80 Interestingly, BRCT domains that contain PBPs are always found in the multi-
81 module configuration, and this is because BRCT::BRCT packing is considered
82 important for formation of the PBP (Leung and Glover, 2011; Reinhardt and Yaffee,
83 2013; Day et al, 2021).

84

85 One previously identified feature of BRCT domains is that they can bind to
86 one another. For example, the XRCC1 BRCT2 domain can form homodimers, as well
87 as heterodimers with the BRCT domain from DNA ligase III (London, 2020). This is
88 also true of TOPBP1, which contains nine BRCT domains. We have recently shown
89 that TOPBP1's BRCT1&2 domains can dimerize, and they can also bind to BRCT5
90 (Kim et al, 2020). Though not as well-studied as interactions involving BRCT
91 domains and phosphorylated substrates, homotypic and heterotypic BRCT::BRCT
92 interactions are likely to be just as important for an efficient DDR. In this work we
93 extend our understanding of BRCT::BRCT interactions by studying how TOPBP1
94 interacts with the NBS1 protein. We chose this interaction to study because recent
95 work from our group showed that NBS1, a component of the critical DNA repair
96 factor MRN, plays an important role in recruiting TOPBP1 to sites of damage
97 (Montales et al, 2022). Here, we report that the NBS1::TOPBP1 interaction is driven
98 by BRCT::BRCT interactions, whereby the BRCT1 domain from NBS1 binds directly
99 to the both the BRCT1 and BRCT2 domains of TOPBP1. Interestingly, NBS1 binds
100 BRCT1 differently than it does BRCT2, with the interaction with BRCT1 using a
101 similar mode of binding as XRCC1::DNA ligase III, and the interaction with BRCT2
102 occurring via what is likely to be a novel mode of BRCT::BRCT interaction. These
103 finding help fill a large knowledge gap in our understanding of how BRCT domain
104 containing proteins can interact with one another.
105

106 **2. Material and Methods**

107 *2.1 Materials*

108 *2.1.1 Plasmids*

109 The expression vector to produce GST-RAD9 Tail has previously been described

110 (Duursma et al., 2013). All other plasmids used in this study are described below, in

111 table format, and all are *Xenopus* proteins. Specific details about plasmid

112 construction are available upon request.

113

Plasmid	Name	Vector	AA coordinates
5Xmyc-BRCT0-2	pHG128	pCS2+MT	1-333
5Xmyc-BRCT0-2 KK155,249EE	pAK42	pCS2+MT	1-333
5Xmyc-BRCT4&5	pJA19	pCS2+MT	480-758
5Xmyc-BRCT0	pHG126	pCS2+MT	1-99
5Xmyc-BRCT1	pHG129	pCS2+MT	100-191
5Xmyc-BRCT2	pJA23	pCS2+MT	191-333
5Xmyc-NBS1	pKM107	pCS2+MT	1-763
5Xmyc-NBS1 1-400	pKM105	pCS2+MT	1-400
5Xmyc-NBS1 1-200	pKR34	pCS2+MT	1-200
5Xmyc-NBS1 100-400	pKR35	pCS2+MT	100-400
5Xmyc-NBS1 1-100	pOH4	pCS2+MT	1-100
5Xmyc-NBS1 100-200	pKR36	pCS2+MT	100-200
5Xmyc-NBS1 200-400	pKR37	pCS2+MT	200-400
5Xmyc-NBS1 393-763	pKM106	pCS2+MT	393-763
MBP-TOPBP1 1-333	pAK53	pUC57-MBP	1-333

MBP-TOPBP1 91-275	pAK56	pUC57-MBP	91-275
MBP-TOPBP1 91-196	pKR23	pUC57-MBP	91-196
MBP-TOPBP1 91-179	pKR24	pUC57-MBP	91-179
MBP-TOPBP1 91-156	pKR25	pUC57-MBP	91-156
MBP-TOPBP1 91-139	pKR26	pUC57-MBP	91-139
MBP-TOPBP1 128-179	pKR29	pUC57-MBP	128-179
MBP-TOPBP1 138-179	pKR30	pUC57-MBP	138-179
MBP-TOPBP1 128-156	pKR38	pUC57-MBP	128-156
MBP	pOH10	pUC57-MBP	-
MBP-TOPBP1 221-273	pOH6	pUC57-MBP	221-273
MBP-TOPBP1 231-273	pOH7	pUC57-MBP	231-273
MBP-TOPBP1 221-250	pOH8	pUC57-MBP	221-250
MBP-TOPBP1 197-231	pOH9	pUC57-MBP	197-231
MBP-TOPBP1 242-273	pOH11	pUC57-MBP	421-273
MBP-TOPBP1 250-273	pOH12	pUC57-MBP	250-273
MBP-TOPBP1 251 - 273 5Am5	pOH26	pUC57-MBP	251 - 273
MBP-TOPBP1 251 - 273 5Am6	pOH27	pUC57-MBP	251 - 273
MBP-TOPBP1 251 - 273 5Am7	pOH28	pUC57-MBP	251 - 273
MBP-TOPBP1 251 - 273 5Am8	pOH29	pUC57-MBP	251 - 273

2.1.2 Recombinant proteins

The recombinant proteins used in this study were GST, GST-NBS1 1-400, GST-NBS1 1-400 K158E, GST-NBS1 393-763, GST-RAD9Tail, GST-BRCT4&5, MBP, MBP-BRCT1&2, and 6His-T7-BRCT0-2. Expression vectors for GST-RAD9Tail (Duursma et al., 2013), GST-BRCT4&5, MBP-BRCT1&2, and 6His-T7-BRCT0-2 (Kim et al, 2020)

120 have been described. Expression vectors for GST-NBS1 1-400, GST-NBS1 1-400
121 K158E, and GST-NBS1 393-763 were made using pGEX4T-2 as the backbone. All
122 proteins were expressed in *E. coli* BL21(DE3) cells, at 37°C for 4 hours, and all
123 proteins were purified from the soluble fraction according to standard procedures
124 (detailed below).
125
126 *2.1.3 Antibodies*
127 We used the following commercially sourced antibodies in this work: Myc
128 (Millipore Sigma #M4439), MBP (New England Biolabs #E8032S), GST (Millipore
129 Sigma #05-782), and T7 (Millipore Sigma #69522). We also used our own antibody
130 against *Xenopus* TOPBP1, HU142, which has been described (Van Hatten et al.,
131 2002).
132
133 *2.2 Methods*
134 *2.2.1 Xenopus egg extracts*
135 Extracts were prepared as previously described (Van Hatten et al., 2002, Yan et al.,
136 2006).
137
138 *2.2.2 IVTT production of proteins and determination of protein concentrations*
139 IVTT reactions were performed using the SP6 TnT® Quick Coupled
140 Transcription/Translation System (Promega #L2080) according to the
141 manufacturer's instructions. For Bug-Bunny binding assays we used 20ul of the
142 IVTT reaction/sample.

143

144 *2.2.3 Recombinant Protein Expression and Purification*

145 Plasmids were transformed in BL21 (DE3) Competent *E. Coli* cells and grown in LB
146 media (GST fusion proteins) or LB media with 0.2% glucose (MBP fusion proteins)
147 with ampicillin. At an OD600 of 0.6-0.8, cells were induced with 0.3 mM IPTG for 4
148 hours at 37˚C. Cells were then harvested by centrifugation (4000 rpm for 20 min)
149 and washed with phosphate-buffered saline (PBS). Cells were lysed by sonication in
150 GST column buffer (40% PBS, 60% TEN buffer: 10 mM Tris-Cl, pH 8.0, 1 mM EDTA,
151 pH 8.0, 100 mM NaCl) supplemented with cOmplete protease inhibitor cocktail
152 tablets (Roche #04693159001) and 10 mg lysozyme for GST fusion proteins or in
153 maltose column buffer (20 mM Tris-HCl, pH 7.4, 0.3 M NaCl, and 1 mM EDTA) with
154 1mM DTT and cOmplete protease inhibitor cocktail tablets for MBP fusion proteins.
155 Lysates were cleared by centrifugation (15,000 rcf for 20 min) and incubated with
156 glutathione sepharose (BioVision #6566) for GST fusion proteins or amylose resin
157 (New England Biolabs #E8021S) for MBP fusion proteins for 1 hour at 4˚C. Beads
158 were poured over a column and washed with column buffer. GST fusion proteins
159 were eluted with 20 mM glutathione in 75 mM HEPES, pH 7.5, 150 mM NaCl, 5 mM
160 DTT, and 0.1% Triton-X. MBP fusion proteins were eluted with 10 mM maltose in
161 maltose column buffer. Proteins were dialyzed overnight into PBS.

162

163 *2.2.4 Protein binding assays*

164 Three kinds of protein binding assays were utilized. The first involved the addition
165 of recombinant proteins to XEE (Figures 1B-D). For these assays 25 ul of XEE was

166 supplemented with 5ug of GST-tagged recombinant protein. DSBs, in the form of
167 EcoRI-digested lambda DNA, were also optionally added (500 ng). After a 30-minute
168 incubation the samples were diluted into 400 ul of Binding Buffer (PBS + 0.1% NP-
169 40) and incubated with glutathione sepharose (BioVision, #6566). The beads were
170 washed four times with 500 ul of Binding Buffer and then eluted with 2X Sample
171 Buffer (Millipore Sigma #S3401-10VL). The total and bound fractions were then
172 analyzed via Western blotting using standard conditions. The second involved
173 incubation of IVTT proteins with recombinant GST or MBP fusion proteins purified
174 from *E. coli,* in what we refer to as the Bugs-Bunny system. For these assays 20 ul of
175 IVTT proteins were mixed with 5 ug of GST or MBP fusion protein and incubated for
176 60 minutes at 30°C. The mixtures were diluted into 400 ul of Binding Buffer and
177 then incubated with the appropriate resin (amylose for MBP, New England Biolabs
178 # E8021S; glutathione sepharose for GST, BioVision #6566) for one hour at 4°C.
179 The beads were washed four times with 500 ul of Binding Buffer and then eluted
180 with 2X Sample Buffer. The input and bound fractions were then analyzed via
181 Western blotting using standard conditions. The third type of binding assay (done
182 once, in Figure 4F) was a variant of the pull-down where MBP recombinant proteins,
183 purified from *E. coli,* were mixed at 10 ug each with 100 ng of 6His-T7-BRCT0-2, also
184 purified from *E. coli.* The samples were then treated as described above for the
185 Bugs-Bunny system.

186 **3. Results**

187 *3.1 The TOPBP1-NBS1 interaction can be recapitulated using E. coli- and IVTT-*
188 *produced proteins.*

189 Previous work from many different laboratories has shown that TOPBP1 and
190 MRN act together to promote DDR signaling, and that NBS1 and TOPBP1 can bind to
191 another (Morishima et al, 2007; Yoo et al, 2009; Duursma et al., 2013; Shiotani et al,
192 2013; Montales et al, 2022). The domain structures of the two proteins are shown in
193 Figure 1A. As detailed above, TOPBP1 contains nine BRCT domains, named 0-8. Of
194 these, BRCT domains 1,2,5, and 7 contain PBPs. NBS1 is less complex, with three
195 protein-protein interaction motifs, two BRCT domains and one FHA domain. For
196 NBS1 the sole PBP is located in BRCT1. One previous study analyzed the interaction
197 between TOPBP1 and NBS1 in some detail (Yoo et al, 2009). Using XEEs, Yoo and
198 colleagues found that TOPBP1 and NBS1 could co-precipitate under resting
199 conditions, and that the interaction was enhanced when DDR signaling was
200 activated. This work went on to show that TOPBP1 uses its BRCT0-2 region to bind
201 NBS1, and that the relevant region within NBS1 mapped to the amino-terminal 400
202 amino acids of the protein. Finally, Yoo and colleagues showed that mutations in the
203 PBPs from both TOPBP1 (BRCT1) and NBS1 (BRCT1) prevented efficient
204 interaction. We have recently shown that MRN is important for recruitment of
205 TOPBP1 to long, linearized dsDNA templates that mimic DSBs (Montales et al,
206 2022). Given these findings, we were motivated to analyze the TOPBP1-NBS1
207 interaction in more detail.

208

209 We first sought to repeat some of the earlier findings by Yoo and colleagues
210 (Yoo et al, 2009), that a fragment of NBS1 corresponding to amino acids 1-400 could
211 bind TOPBP1 after incubation in XEE. Accordingly, we expressed and purified from
212 *E. coli* two GST-NBS1 1-400 fusion proteins, one corresponding to the wild type
213 sequence and the other containing a K158E mutation that attenuates the PBP in
214 BRCT1 of NBS1 (Figure 1A). These proteins, along with GST alone, were added to
215 XEE in either the presence or absence of linearized 5kb dsDNA, which we have
216 previously shown will potently activate both ATR and ATM in our XEEs (Montales et
217 al, 2021; Ruis et al, 2022; Montales et al, 2022). The GST protein complexes were
218 then recovered back out of the XEE using glutathione-sepharose beads, and the
219 presence of endogenous TOPBP1 was detected via Western blotting. As displayed in
220 Figure 1B, TOPBP1 did not bind to GST alone, but it did bind well to the wild type
221 form of GST-NBS1 1-400. Binding was clearly evident in the sample lacking DSBs,
222 and was enhanced by the presence of DSBs. By contrast, binding to the K158E form
223 of GST-NBS1 1-400 was severely attenuated, under both -DSB and +DSB conditions
224 (Figure 1B). We next asked if there are additional binding sites for TOPBP1 within
225 NBS1, beyond those present in the 1-400 region. We found that this is not likely, as
226 TOPBP1 did not bind to a GST fusion containing NBS1 from residue 393 to the end
227 of the protein, amino acid 763 (Figure 1C). Lastly, we wanted to confirm that the
228 BRCT0-2 region of TOPBP1 could bind to NBS1 1-400, and for this a myc-tagged
229 TOPBP1 fragment corresponding to BRCT0-2 was produced by *in vitro* transcription
230 and translation (IVTT) and added to XEE along with GST-NBS1 1-400. DSBs were
231 optionally added, and we observed that myc-TOPBP1 BRCT0-2 could readily bind to

232 GST-NBS1 1-400, but not to GST alone, and that binding was modestly enhanced by
233 DSBs (Figure 1D). Taken together, the data in Figures 1B-D are all in excellent
234 agreement with prior work of Yoo et al (Yoo et al, 2009). We note that neither full-
235 length TOPBP1 nor the myc-tagged BRCT0-2 fragment can bind to GST alone
236 (Figures 1B,D; see also Kim et al, 2020), and thus moving forward we did not include
237 the GST alone control for every experiment.
238
239 Previous work, and data shown here, reveal that there is a constitutive, or
240 basal, interaction between TOPBP1 and NBS1 that occurs in XEE even in the absence
241 of DDR signaling (Figures 1B-D; Yoo et al, 2009). We wanted to study this basal
242 interaction further, and we first asked if we could recapitulate it using a protein-
243 binding assay that we nicknamed Bugs-Bunny (Figure 2A). In the Bugs-Bunny
244 system one binding partner is expressed and purified from *E. coli* (Bugs) and the
245 other is synthesized by IVTT in rabbit reticulocyte lysates (Bunny). After synthesis
246 of one binding partner in the IVTT reaction we simply add the purified form of the
247 other partner to the rabbit reticulocyte lysates. After incubation the samples are
248 diluted in binding buffer and protein complexes isolated using an affinity resin
249 corresponding to the tag on the *E. coli* produced protein (for this study the tag is
250 predominantly GST, but sometimes MBP). This system has several advantages for
251 the study of protein-protein interactions. One, the endogenous proteins present in
252 the reticulocyte lysates help to prevent non-specific binding of the target protein to
253 the resin. Two, as detailed below, the reticulocyte lysates can contain modifying
254 enzymes, such as casein kinase 2 (CK2), that are important for certain interactions.

255 Three, and most importantly, because synthesis of a target protein by IVTT is far
256 less labor intensive than purification of the target from bacterial or insect cells, one
257 can rapidly screen through a collection of mutants to analyze sequence
258 determinants required for the interaction. Lastly, in our experience, proteins are
259 much better behaved, in terms of proper folding and solubility, when made by IVTT
260 relative to other expression systems.
261
262 We first examined binding of GST-NBS1 1-400 to myc-tagged TOPBP1
263 BRCT0-2 in the Bugs-Bunny assay. As shown in Figure 2B, myc-BRCT0-2 could bind
264 to wild type GST-NBS1 1-400 under these assay conditions, and binding was greatly
265 reduced when the K158A form of NBS1 was used. These data show that the
266 NBS1::TOPBP1 interaction is readily observed using the Bugs-Bunny system, and
267 thus that XEE is not required for the interaction to occur. We also asked if the PBP
268 pockets within TOPBP1's BRCT1 and 2 domains are required for the interaction, by
269 testing the "EE" mutant, where the conserved lysines (K155 and K249) within the
270 PBPs of both BRCT1 and BRCT2 had been mutated to glutamic acid (Figure 1A). We
271 found that the EE mutant binds as efficiently as wild type to NBS1 (Figure 2B). Thus,
272 the NBS1::TOPBP1 interaction, as it occurs in the Bugs-Bunny system, requires the
273 NBS1 PBP, but not those of TOPBP1. We next assessed the specificity of the
274 interaction between NBS1 and TOPBP1's BRCT0-2 region by asking if NBS1 could
275 also bind to TOPBP1's BRCT4&5 domains. Binding assays were run with the
276 following partners: GST-NBS1 1-400 with myc-tagged TOPBP1 BRCT0-2 or 4&5
277 domains, and GST fused to the RAD9 Tail domain (RAD9Tail) with the same pair of

278 TOPBP1 proteins. We included RAD9Tail because we had previously shown that it
279 binds well to myc-BRCT0-2 in our Bugs-Bunny system (Kim et al, 2020). As shown
280 in Figure 2C, myc-BRCT0-2 could bind as efficiently to NBS1 as it did to the
281 RAD9Tail, and myc-BRCT4&5 failed to bind efficiently to either NBS1 or RAD9Tail.
282 We conclude that the Bugs-Bunny system faithfully recapitulates a specific
283 interaction between NBS1 and TOPBP1.
284
285 Because the NBS1::TOPBP1 interaction requires the NBS1 BRCT1 PBP, we
286 were curious if the interaction was dependent on phosphorylation. Previous work
287 from our group has shown that the interaction between TOPBP1 and the RAD9Tail,
288 which requires phosphorylation of RAD9Tail, can be recapitulated in the Bugs-
289 Bunny system and this is because the reticulocyte lysates used for IVTT contain CK2,
290 the kinase responsible for RAD9Tail phosphorylation (Kim et al, 2020). Myc-BRCT0-
291 2 was produced by IVTT and, prior to addition of the GST fusion proteins, the
292 samples were optionally treated with lambda phosphatase. As expected,
293 phosphatase treatment eliminated the RAD9Tail::TOPBP1 interaction, however the
294 NBS1::TOPBP1 interaction was refractory to phosphatase treatment (Figure 2D).
295 We conclude that, despite the requirement for the NBS1 BRCT1 PBP, the
296 NBS1::TOPBP1 interaction does not require the presence of phosphate on TOPBP1.
297
298 *3.2 NBS1 can bind to both BRCT1 and BRCT2 of TOPBP1*
299 To pursue these observations, we next asked if NBS1 required an intact BRCT0-2
300 region for binding to TOPBP1. To explore this, we subdivided TOPBP1's BRCT0-2

301 region into the individual BRCT domains and tested them for binding to NBS1.
302 Surprisingly, both BRCT1 and BRCT2 could bind to NBS1 (Figure 3A), whereas
303 BRCT0 could not. Efficient binding of either BRCT1 or BRCT2 to NBS1 was
304 dependent on NBS1 K158 (Figure 3B), demonstrating that the interactions are
305 specific and not the result of the isolated BRCT1 or BRCT2 domains becoming
306 "sticky" proteins upon separation from one another. In addition, while NBS1 readily
307 binds the isolated BRCT1 or BRCT2 domains, the same is not true of RAD9Tail, as it
308 could only interact with the contiguous BRCT0-2 region, and not the individual
309 BRCT1 or BRCT2 domains (Figure 3C). Taken together, the data presented in
310 Figures 1-3 show that the TOPBP1 BRCT0-2 region interacts with NBS1 in a
311 fundamentally different manner than it does with RAD9Tail. The RAD9Tail::TOPBP1
312 interaction requires an intact BRCT0-2 region and is dependent on phosphorylation
313 (summarized in Figure 3D), whereas the NBS1::TOPBP1 interaction requires neither
314 an intact BRCT0-2 region nor phosphorylation (Figure 3E).
315
316 *NBS1 uses its BRCT1 domain to bind directly to TOPBP1.*
317 Having determined that BRCT1 or BRCT2 from TOPBP1 are both capable of
318 binding to NBS1 we next flipped the problem on its head and asked which domains
319 within NBS1 1-400 could bind TOPBP1. The constructs used for this are
320 summarized in Figure 4A. We first wanted to confirm that full-length NBS1 could
321 bind TOPBP1's BRCT1&2 domains in the Bugs-Bunny system, and to do so we
322 employed an MBP-BRCT1&2 fusion protein purified from E. coli, together with myc-
323 tagged NBS1, made by IVTT. As shown in Figure 4B, full-length myc-NBS1 can bind

324 MBP-BRCT1&2, but not MBP alone. Given that full-length NBS1 is incapable of
325 binding to MBP alone, moving forward we did not include the MBP alone control in
326 all experiments. We also observed that MBP-BRCT1&2 could bind the NBS1 1-400
327 region, but not the 393-763 region (Figure 4C). These data show that despite
328 switching production of the TOPBP1 region from IVTT to E. coli, and vise-versa for
329 NBS1, the specificity of the interaction was not altered. We next used MBP-BRCT1&2
330 to delineate the region within NBS1 to which it binds. We found that myc-tagged
331 NBS1 1-400 bound well, as expected (Figure 4D). A smaller fragment, amino acids 1-
332 200 and comprised of the FHA domain plus BRCT1, also bound well to MBP-
333 BRCT1&2. Further delineation revealed that loss of the FHA domain did not alter
334 binding, as a fragment containing just the two BRCT domains could bind to
335 TOPBP1's BRCT1&2 domains (Figure 4D). Interestingly, when the two BRCT
336 domains were tested for binding in isolation, we saw that BRCT1 could bind well,
337 but BRCT2 showed no detectable binding. The data in Figure 4D show clearly that
338 NBS1 BRCT1 can interact with TOPBP1 BRCT1&2, and that NBS1 BRCT2 cannot, but
339 they left open the possibility that the FHA domain could bind TOPBP1 BRCT1&2. To
340 explore this we ran the experiment shown in Figure 4E. Unlike NBS1 BRCT1, the
341 FHA domain showed no detectable binding to TOPBP1. We conclude that it is
342 BRCT1 from NBS1 that mediates the interaction with TOPBP1's BRCT1 or BRCT2
343 domains.
344
345 Having defined the region of NBS1 that binds TOPBP1, we next asked if the
346 NBS1::TOPBP1 interaction is direct, or if it requires a bridging factor that might be

347 present in the reticulocyte lysates used for our binding assays. For this we
348 expressed and purified an MBP-NBS1 1-200 fusion protein from E. coli. We initially
349 attempted to purify MBP-NBS1 100-200, however we found that this fusion protein
350 was insoluble and difficult to express in E. coli. We also produced a 6His-T7-TOPBP1
351 BRCT0-2 recombinant protein, one that we have used in the past (Kim et al, 2020).
352 Thus, in this experiment, both proteins were expressed in E. coli and then purified,
353 thereby eliminating concerns about bridging factors. To block non-specific binding
354 to the resin the assays were performed in binding buffer supplemented with 1%
355 BSA. As shown in Figure 4F, 6His-T7-TOBP1 BRCT0-2 could readily bind MBP-NBS1
356 1-200, but not MBP alone. We conclude that the interaction between NBS1 and
357 TOPBP1 is direct and does not require any post-translational modifications on
358 either partner.
359
360 *3.4 A 29 amino-acid sequence in the central region of TOPBP1 BRCT1 promotes*
361 *binding to NBS1 in a transferrable manner.*
362 To learn more about the NBS1::TOPBP1 interaction we decided to identify the
363 sequences within the TOPBP1 BRCT1 and 2 domains that mediate the interaction.
364 To do so we engineered a system whereby MBP fusions proteins could be rapidly
365 produced by IVTT and then used in binding assays with GST-NBS1 1-400. Figure 5A
366 shows the constructs used for the delineation analysis. As shown in Figure 5B, we
367 found that all constructs that contained an intact BRCT1 domain would bind to
368 NBS1, showing that the NBS1-binding capacity of BRCT1 can be transferred to a
369 heterologous protein (MBP). Further delineation within BRCT1 revealed the

370 following results: we found that while a fragment corresponding to amino acids 91-
371 156 could bind NBS1, a slightly smaller fragment, amino acids 91-139, could not
372 bind (Figure 5C). Thus, the C-terminal border of the NBS1 binding region,
373 operationally defined, is amino acid 156. We then came in from the N-terminal side
374 and observed that a fragment running from amino acids 128 to 179 could bind
375 NBS1, but the fragment from amino acids 138-179 could not (Figure 5D). This
376 operationally establishes the N-terminal border at position 128. Finally, we asked if
377 a fragment corresponding to the two borders, 128 to 156, retained the capacity to
378 bind NBS1 and we found that it did (Figure 5E). These data show that, surprisingly,
379 an intact BRCT1 domain is dispensable for the NBS1 interaction, and that the ability
380 to bind NBS1 is encoded by a small, 29 amino-acid sequence centrally located within
381 the domain. We have named this sequence NBR1 for NBS-binding region 1 (Figure
382 5F). Interestingly, previous work has shown that the interaction between the BRCT2
383 domain of XRCC1 and the BRCT domain of DNA ligase III depends on a similar
384 sequence in XRCC1 as the TOPBP1 NBR1 (Taylor et al, 1998). As detailed in the
385 Discussion, these data suggest that the TOPBP1 BRCT1::NBS1 BRCT1 interaction is
386 mechanistically similar to the well-studied XRCC1 BRCT2::DNA ligase III BRCT
387 interaction.
388
389 *3.5 A novel mode of BRCT::BRCT interaction for binding of NBS1 to TOPBP1 BRCT2.*
390 We next examined BRCT2 and going into this we expected that its NBR would
391 be analogous to the BRCT1 NBR1, i.e. centrally located. This, however, was not the
392 case. Figure 6A shows the constructs used for the BRCT2 analysis, and the construct

393 that corresponds to the central region is 221-250. As shown in Figure 6B, this
394 construct could not bind to NBS1, and in the same experiment we see again that the
395 central region of BRCT1, amino acids 128-156, does bind to NBS1. In addition, we
396 observed that a fragment corresponding to the N-terminal half of BRCT2, amino
397 acids 197-231, also failed to bind (Figure 6B). This focused attention on the C-
398 terminal portion of BRCT2, and we found through a series of N-terminal truncations
399 that we could remove most of the N-terminal BRCT2 sequences and still retain
400 binding to NBS1 (Figures 6C&D). These data show that a small, 24-amino acid
401 region at the extreme C-terminus of BRCT2, running from amino acids 250 to 273, is
402 sufficient to confer binding to NBS1 (Figure 6E). We named this motif NBR2.
403
404 We next wanted to determine which amino acids within TOPBP1's NBR2 are
405 required for binding to NBS1. For this analysis we systematically mutated all but
406 two residues within NBR2 to alanine, and we did so in blocks of 5 or 6 amino acids
407 (Figure 6F). These mutations were introduced in the context of the full BRCT2
408 domain (amino acids 197-296) fused to MBP. As shown in Figures 6G, mutation of
409 the extreme C-terminal and N-terminal blocks did not disrupt binding to NBS1. By
410 contrast, mutation of the internal blocks did impact binding (Figure 6H), and one
411 mutant (aa 263-268) showed substantially reduced binding. These data show that
412 that the key residues mediating association of BRCT2 with NBS1 are amino acids
413 256-268.
414

415 *3.6 Binding of TOPBP1 BRCT1 and BRCT2 to TOPBP1 BRCT 4&5 relies on the same*
416 *motifs that are needed to bind NBS1.*
417 Previous work from our group had shown that TOPBP1 self-associates via an
418 array of BRCT::BRCT domain interactions (Kim et al, 2020). In this previous work
419 we showed that the BRCT 1&2 pair can bind isolated BRCT domains 1,2, and 5, and
420 that the BRCT4&5 pair can bind to isolated BRCT domains 1 and 2. Data shown here
421 demonstrate that NBS1 can bind to isolated BRCT domains 1 and 2 as well, and thus
422 it was of interest to see if the same determinants used by BRCT1 and BRCT2 to bind
423 NBS1 are also required for binding to BRCT4&5. As shown in Figure 7A, the MBP-
424 BRCT1 91-156 construct could bind to GST-BRCT4&5, but not to GST alone. The 91-
425 139 fragment failed to bind GST-BRCT4&5, while the minimally defined region for
426 NBS1 binding, 128-156, did bind. This is the same pattern of binding/not binding
427 that was observed for NBS1 (Figure 5), and thus we conclude that BRCT1 uses the
428 same motif, NBR1, to bind both NBS1 and TOPBP1 BRCT4&5. For BRCT2, we found
429 that the minimally defined region for NBS1 binding, amino acids 250-273, was not
430 sufficient to bind BRCT4&5 (Figures 7B); however, a slightly larger fragment
431 corresponding to amino acids 242-273 did bind. Thus, BRCT2 requires a handful of
432 additional N-terminal amino acids to bind BRCT4&5, relative to NBS1, but
433 nonetheless the determinants are largely overlapping (Figure 7C).
434

435 **4. Discussion**

436 BRCT domain containing proteins are major players in the cellular response
437 to DNA damage and, as such, it is crucial that we understand how they function and
438 that we fully describe all the different modes by which they interact with their
439 binding partners. Two BRCT proteins that are at the heart of the DDR are TOPBP1
440 and NBS1. They are known to bind one another, and this interaction is conserved
441 from frogs to man (Morishima et al, 2007; Yoo et al, 2009). Interestingly, in both
442 frogs and humans, TOPBP1 and NBS1 constitutively bind to one another, and the
443 interaction is then enhanced during the DDR (Morishima et al, 2007; Yoo et al,
444 2009). In this study we analyzed the constitutive interaction using the Bugs-Bunny
445 assay system. It was important to ensure that the NBS1-TOPBP1 interaction could
446 be faithfully recapitulated in Bugs-Bunny. Data in support of a specific interaction
447 include the finding that the NBS1 K158E point mutation abrogates the interaction in
448 Bugs-Bunny (Figure 2B), as it does in XEE (Figure 1B and Yoo et al, 2009).
449 Furthermore, NBS1 does not bind TOPBP1's BRCT4&5 domains (Figure 2C),
450 showing that it is not non-specifically interacting with just any BRCT domain. In
451 addition, TOPBP1's BRCT1&2 domains are highly selective for the NBS1 BRCT1
452 domain, as binding to the NBS1 BRCT2 or FHA domains is undetectable (Figures
453 4D&E). Thus, Bugs-Bunny can reveal highly specific interactions, and is thereby
454 suitable for a detailed analysis of the TOPBP1-NBS1 interaction.

455

456 Our data support the conclusion that the NBS1 BRCT1 domain can bind
457 directly to both TOPBP1's BRCT1 and BRCT2 domains, and that these interactions

458 allow NBS1 to bind TOPBP1 in a non-regulated, constitutive manner. There are
459 several intriguing questions that emerge from this discovery. First, why would
460 evolution select for two distinct binding sites for NBS1 on TOPBP1? Both
461 interactions rely on NBS1 K158, and, therefore, it is not the case that NBS1 also has
462 two binding sites for TOPBP1, as NBS1 likely uses the same interface for both
463 interactions. It thus appears that NBS1 can occupy one or the other binding site on
464 TOPBP1, or perhaps two molecules of NBS1 can simultaneously engage TOPBP1 via
465 the two binding sites. It is also curious that K158, which is part of the NBS1 BRCT1
466 PBP, is required for binding, however phosphate is not (Figure 2D). One possibility
467 is that, under resting conditions, the interaction between NBS1 and TOPBP1 serves
468 to mask the NBS1 PBP, and thereby prevents spurious and/or inappropriate
469 interactions with phosphorylated proteins. We note that our data show no
470 requirement for the PBPs present in TOPBP1 BRCT1 or BRCT2 for the interaction
471 with NBS1 (Figure 2B). For this experiment we mutated the conserved lysine
472 residues within the two PBPs to glutamic acid, and in data not shown we confirmed
473 that this mutant cannot bind to the RAD9Tail. We note that Yoo and colleagues
474 mutated the same lysine in BRCT1 (K155) that we did, but they also mutated the
475 neighboring lysine (K154) to generate a KK->AM mutant. They observed that
476 binding to NBS1 was attenuated by these mutations (Yoo et al, 2009). One
477 explanation for this discrepancy is that mutation of both lysines (K154 & K155) in
478 BRCT1 is needed to observe a defect in binding.
479

480 One important finding revealed by our work is the remarkable versatility
481 that TOPBP1's BRCT0-2 region displays in its interactions with various binding
482 partners. On the one hand, there is the well-studied, phosphate-dependent
483 interaction with RAD9Tail (and other phospho-substrates), and on the other hand,
484 as we have shown here, is a very different mode of interaction, involving phosphate-
485 free and direct binding to NBS1. There are important differences between the
486 phosphate-dependent and phosphate-free modes of binding. For the former, a
487 contiguous BRCT0-2 module is required for efficient binding. In the case of the
488 RAD9Tail, previous work has shown that it is BRCT1 that contacts phosphate
489 (Rappas et al, 2011), however BRCT1 alone is not sufficient for the interaction
490 (Figure 3C), and in data not shown we have observed that BRCT0 also plays a
491 positive role, as the BRCT0-2 region binds RAD9Tail more efficiently than does the
492 BRCT1&2 region. Thus, the BRCT0-2 continuum is needed for optimal binding in the
493 phosphate -dependent mode, and nothing could be further from the truth for the
494 phosphate-independent mode. All that is required for the phosphate-independent
495 mode are relatively small sequences within the BRCT domains. These sequences,
496 termed NBR1 and NBR2, are <30 amino acids and both can be transferred to
497 heterologous proteins such as MBP to allow binding to NBS1.
498
499 A critical question that arises from our studies is how NBR1 and NBR2
500 mediate the interaction with NBS1. NBR1 maps to the α1-β2-β3 region of BRCT1
501 (Figures 8A&B). Importantly, previous work on the XRCC1 BRCT2::DNA ligase III
502 BRCT interaction had shown that a similar region is used by XRCC1 BRCT2 to bind

503 DNA ligase III (Taylor et al, 1998; Dulic et al, 2001; Cuneo et al, 2011; Hammel et al,
504 2021). Furthermore, just like TOPBP1 BRCT1, a short peptide sequence from the
505 analogous position in XRCC1 can mediate binding to DNA ligase III upon transfer to
506 a heterologous protein (Taylor et al, 1998). In Figure 8C this sequence is underlined
507 in black, it maps to the β2-β3 region of XRCC1, just as NBR1 maps to the β2-β3
508 region of TOPBP1's BRCT1. Extensive structural analysis has defined the interface
509 that XRCC1 uses to bind DNA ligase III, and it is largely produced by the C-terminal
510 portion of α1 extending into and beyond β2 (Cuneo et al, 2011; Hammel et al, 2021).
511 Mutagenesis experiments have shown that residues positioned in the C-terminal
512 region of XRCC1 BRCT2's α1 contribute to the binding (shown in red in Figure 8C),
513 even though they are not required in the context of the short peptide that confers
514 binding to heterologous proteins. Given this, it is likely that, within the context of
515 the properly folded domain, TOPBP1's BRCT1 also relies on a more substantial
516 interface than what is represented by NBR1 to bind to NBS1. Nonetheless, for both
517 XRCC1 BRCT2 and TOPBP1 BRCT1, the small transferrable regions retain enough of
518 the interface to allow binding. This has important implications for the design of
519 peptide modifiers that can potentially disrupt BRCT::BRCT interactions and thereby
520 impact DDR signaling, possibly in a therapeutic manner.
521
522 Recent data have examined how ECT2, the only other triplet BRCT containing
523 protein besides TOPBP1, binds to its partner CYK4 (Gómez-Cavazos et al, 2020). In
524 this scenario, ECT2 uses its BRCT1 domain to bind CYK4 that has been
525 phosphorylated by PLK – however, despite the requirement for phosphate, the PBP

526 within ECT2 is dispensable for binding. Instead, ECT2 uses a negatively charged
527 interface located in the central, β2-β3 region of BRCT1. Figure 8D shows an
528 alignment of the BRCT1 domains from TOPBP1 and ECT2 and shown in red coloring
529 are three basic amino acids in the ECT2 domain that mediate binding to CYK4. Note
530 that despite good overall conservation between these two BRCT domains the basic
531 residues are not found in TOPBP1, and thus it is unlikely that the analogous
532 interface in TOPBP1 BRCT2 is able to interact with phosphate. In summary, data
533 presented here together with previous work show that a binding interface located in
534 the central, α1-β2-β3 region of certain BRCT domains can mediate BRCT::BRCT
535 interactions, in the case of XRCC1 and TOPBP1, and phosphate-dependent
536 interactions in the case of ECT2.
537
538 It is presently unclear how NBR2 mediates its interaction with NBS1, as there
539 are no precedents (to our knowledge) for a BRCT domain to utilize its extreme C-
540 terminal region for interaction with a heterologous BRCT domain. NBR2 is well
541 conserved in human TOPBP1, with only one non-conservative substitution (Figure
542 8D). This 95.8% similarity is substantially higher than the overall similarity between
543 human and frog TOPBP1 (66%) and is also higher than the similarity between the
544 BRCT2 domains (79%), strongly suggesting a conservation of function. A similar but
545 less dramatic pattern is observed when comparing frog TOPBP1 to its Drosophila
546 ortholog, MUS-101. The NBR2 region shows 45.8% conservation (Figure 8E),
547 whereas conservation drops to 37.6% when comparing the entire BRCT2 domains.

548 Future studies will address the possibility that the NBR2 mode of BRCT::BRCT

549 interaction is found in other binding partners or if it is unique to TOPBP1::NBS1.

550 **Author contribution**

551 W.M.M. conceptualized the project, acquired the funding, and wrote the manuscript

552 together with O.H. O.H., K.R., and K.M. performed the experiments.

553

554 **Conflict of interest statement**

555 The authors declare no conflict of interest.

556

557 **Acknowledgments**

558 This work was supported by NIH grant R01GM12287. We thank Karlene Cimprich

559 for the gift of the GST-RAD9 Tail expression vector.

560 **References**
561
562 Bagge J, Oestergaard VH, Lisby M. Functions of TopBP1 in preserving genome
563 integrity during mitosis. Semin Cell Dev Biol. 2021 May;113:57-64. doi:
564 10.1016/j.semcdb.2020.08.009.
565
566 Bigot N, Day M, Baldock RA, Watts FZ, Oliver AW, Pearl LH. Phosphorylation-
567 mediated interactions with TOPBP1 couple 53BP1 and 9-1-1 to control the G1 DNA
568 damage checkpoint. Elife. 2019 May 28;8:e44353. doi: 10.7554/eLife.44353.
569
570 Costa A, Diffley JFX. The Initiation of Eukaryotic DNA Replication. Annu Rev
571 Biochem. 2022 Jun 21;91:107-131. doi: 10.1146/annurev-biochem-072321-110228.
572
573 Cuneo MJ, Gabel SA, Krahn JM, Ricker MA, London RE. The structural basis for
574 partitioning of the XRCC1/DNA ligase III-α BRCT-mediated dimer complexes.
575 Nucleic Acids Res. 2011 Sep 1;39(17):7816-27. doi: 10.1093/nar/gkr419.
576
577 Day M, Oliver AW, Pearl LH. Phosphorylation-dependent assembly of DNA damage
578 response systems and the central roles of TOPBP1. DNA Repair (Amst). 2021
579 Dec;108:103232. doi: 10.1016/j.dnarep.2021.103232.
580
581 Dulic A, Bates PA, Zhang X, Martin SR, Freemont PS, Lindahl T, Barnes DE. BRCT
582 domain interactions in the heterodimeric DNA repair protein XRCC1-DNA ligase III.
583 Biochemistry. 2001 May 22;40(20):5906-13. doi: 10.1021/bi002701e.
584
585 Duursma AM, Driscoll R, Elias JE, Cimprich KA. A role for the MRN complex in ATR
586 activation via TOPBP1 recruitment. Mol Cell. 2013 Apr 11;50(1):116-22. doi:
587 10.1016/j.molcel.2013.03.006.
588
589 Gómez-Cavazos JS, Lee KY, Lara-González P, Li Y, Desai A, Shiau AK, Oegema K. A
590 Non-canonical BRCT-Phosphopeptide Recognition Mechanism Underlies RhoA
591 Activation in Cytokinesis. Curr Biol. 2020 Aug 17;30(16):3101-3115.e11. doi:
592 10.1016/j.cub.2020.05.090.
593
594 Hammel M, Rashid I, Sverzhinsky A, Pourfarjam Y, Tsai MS, Ellenberger T, Pascal JM,
595 Kim IK, Tainer JA, Tomkinson AE. An atypical BRCT-BRCT interaction with the
596 XRCC1 scaffold protein compacts human DNA Ligase IIIα within a flexible DNA
597 repair complex. Nucleic Acids Res. 2021 Jan 11;49(1):306-321. doi:
598 10.1093/nar/gkaa1188.
599
600 Hou WH, Chen SH, Yu X. Poly-ADP ribosylation in DNA damage response and cancer
601 therapy. Mutat Res Rev Mutat Res. 2019 Apr-Jun;780:82-91. doi:
602 10.1016/j.mrrev.2017.09.004.
603

604 Kim A, Montales K, Ruis K, Senebandith H, Gasparyan H, Cowan Q, Michael WM.
605 Biochemical analysis of TOPBP1 oligomerization. DNA Repair (Amst). 2020
606 Dec;96:102973. doi: 10.1016/j.dnarep.2020.102973.
607
608 Leung CC, Glover JN. BRCT domains: easy as one, two, three. Cell Cycle. 2011 Aug
609 1;10(15):2461-70. doi: 10.4161/cc.10.15.16312.
610
611 London RE. XRCC1 - Strategies for coordinating and assembling a versatile DNA
612 damage response. DNA Repair (Amst). 2020 Sep;93:102917. doi:
613 10.1016/j.dnarep.2020.102917.
614
615 Ma M, Rodriguez A, Sugimoto K. Activation of ATR-related protein kinase upon DNA
616 damage recognition. Curr Genet. 2020 Apr;66(2):327-333. doi: 10.1007/s00294-
617 019-01039-w.
618
619 Montales K, Kim A, Ruis K, Michael WM. Structure-function analysis of TOPBP1's
620 role in ATR signaling using the DSB-mediated ATR activation in Xenopus egg
621 extracts (DMAX) system. Sci Rep. 2021 Jan 11;11(1):467. doi: 10.1038/s41598-020-
622 80626-1.
623
624 Montales K, Ruis K, Lindsay H, Michael WM. MRN-dependent and independent
625 pathways for recruitment of TOPBP1 to DNA double-strand breaks. PLoS One. 2022
626 Aug 2;17(8):e0271905. doi: 10.1371/journal.pone.0271905.
627
628 Morishima K, Sakamoto S, Kobayashi J, Izumi H, Suda T, Matsumoto Y, Tauchi H, Ide
629 H, Komatsu K, Matsuura S. TopBP1 associates with NBS1 and is involved in
630 homologous recombination repair. Biochem Biophys Res Commun. 2007 Nov
631 3;362(4):872-9. doi: 10.1016/j.bbrc.2007.08.086.
632
633 Moudry P, Watanabe K, Wolanin KM, Bartkova J, Wassing IE, Watanabe S, Strauss R,
634 Troelsgaard Pedersen R, Oestergaard VH, Lisby M, Andújar-Sánchez M, Maya-
635 Mendoza A, Esashi F, Lukas J, Bartek J. TOPBP1 regulates RAD51 phosphorylation
636 and chromatin loading and determines PARP inhibitor sensitivity. J Cell Biol. 2016
637 Feb 1;212(3):281-8. doi: 10.1083/jcb.201507042.
638
639 Rappas M, Oliver AW, Pearl LH. Structure and function of the Rad9-binding region of
640 the DNA-damage checkpoint adaptor TopBP1. Nucleic Acids Res. 2011
641 Jan;39(1):313-24. doi: 10.1093/nar/gkq743.
642
643 Reinhardt HC, Yaffe MB. Phospho-Ser/Thr-binding domains: navigating the cell
644 cycle and DNA damage response. Nat Rev Mol Cell Biol. 2013 Sep;14(9):563-80. doi:
645 10.1038/nrm3640.
646
647 Ruis K, Huynh O, Montales K, Barr NA, Michael WM. Delineation of a minimal
648 topoisomerase II binding protein 1 for regulated activation of ATR at DNA double-
649 strand breaks. J Biol Chem. 2022 Jul;298(7):101992. doi:10.1016/j.jbc.2022.101992.

650
651 Sheng ZZ, Zhao YQ, Huang JF. Functional Evolution of BRCT Domains from Binding
652 DNA to Protein. Evol Bioinform Online. 2011;7:87-97. doi: 10.4137/EBO.S7084.
653
654 Shiotani B, Nguyen HD, Håkansson P, Maréchal A, Tse A, Tahara H, Zou L. Two
655 distinct modes of ATR activation orchestrated by Rad17 and Nbs1. Cell Rep. 2013
656 May 30;3(5):1651-62. doi: 10.1016/j.celrep.2013.04.018.
657
658 Taylor RM, Wickstead B, Cronin S, Caldecott KW. Role of a BRCT domain in the
659 interaction of DNA ligase III-alpha with the DNA repair protein XRCC1. Curr Biol.
660 1998 Jul 16;8(15):877-80. doi: 10.1016/s0960-9822(07)00350-8.
661
662 Van Hatten RA, Tutter AV, Holway AH, Khederian AM, Walter JC, Michael WM. The
663 Xenopus Xmus101 protein is required for the recruitment of Cdc45 to origins of
664 DNA replication. J Cell Biol. 2002 Nov 25;159(4):541-7. doi:
665 10.1083/jcb.200207090.
666
667 Wan B, Hang LE, Zhao X. Multi-BRCT scaffolds use distinct strategies to support
668 genome maintenance. Cell Cycle. 2016 Oct;15(19):2561-2570. doi:
669 10.1080/15384101.2016.1218102.
670
671 Wardlaw CP, Carr AM, Oliver AW. TopBP1: A BRCT-scaffold protein functioning in
672 multiple cellular pathways. DNA Repair (Amst). 2014 Oct;22:165-74. doi:
673 10.1016/j.dnarep.2014.06.004.
674
675 Yan S, Lindsay HD, Michael WM. Direct requirement for Xmus101 in ATR-mediated
676 phosphorylation of Claspin bound Chk1 during checkpoint signaling. J Cell Biol.
677 2006 Apr 24;173(2):181-6. doi: 10.1083/jcb.200601076.
678
679 Yoo HY, Kumagai A, Shevchenko A, Shevchenko A, Dunphy WG. The Mre11-Rad50-
680 Nbs1 complex mediates activation of TopBP1 by ATM. Mol Biol Cell. 2009
681 May;20(9):2351-60. doi: 10.1091/mbc.e08-12-1190.

682 **Figures and Legends**

683

684 **Figure 1. NBS1 binds to TOPBP1 in a manner dependent on K158 of NBS1.**

685 **A.** Schematic representation of the proteins of interest. TOPBP1 contains 9 BRCT

686 domains, four of which contain PBPs. NBS1 contains two BRCT domains, one of

687 which harboring a PBP, as well as an N-terminal FHA domain. In this study we

688 mutated two of the TOPBP1 PBPs and the sole PBP in NBS1, as depicted by the K->E

689 symbols **B.** Either GST or GST-NBS1 recombinant proteins (5 ug) were added to

690 25ul of XEE as indicated. EcoRI-digested lambda DNA (referred to as "DSBs", 500 ng,

691 see Montales et al, 2020) was also included, as indicated. After a 30-minute

692 incubation the samples were diluted in binding buffer and incubated with

693 glutathione-sepharose beads. The beads were washed and bound proteins then

694 eluted and probed by Western blot for the presence of TOPBP1 and the GST

695 proteins, as indicated. A sample of the total extract, taken prior to dilution of the

696 samples, was also probed for TOPBP1 (panel "total"). The experiment shown is

697 representative of two independently performed biological replicates. **C.** Same as (B)

698 except GST-NBS1 393-763 was utilized. The experiment shown is representative of

699 two independently performed biological replicates. **D.** Either GST or GST-NBS1

700 recombinant proteins (5 ug) were added to 25ul of XEE as indicated. Myc-tagged

701 TOPBP1 BRCT0-2, produced by IVTT, was also added (2.5 ul of the IVTT reaction).

702 EcoRI-digested lambda DNA DSBs (500 ng) was also included, as indicated. The

703 samples were then processed as in (B). The experiment shown is representative of

704 two independently performed biological replicates.

705

706 **Figure 2. The Bugs-Bunny system recapitulates a specific, phosphate-**

707 **independent interaction between NBS1 and TOPBP1.**

708 **A.** Overview of the Bugs-Bunny protein binding assay system. **B.** The indicated GST

709 proteins, expressed and purified from *E. coli*, were incubated in IVTT reactions

710 expressing the indicated myc-tagged proteins. The samples were then processed as

711 described in (A). Samples of the total binding reaction, taken prior to dilution, were

712 also probed for myc, showing that the myc-tagged proteins were present in

713 equivalent amounts across all of the samples (lane "input"). The experiment shown

714 is representative of two independently performed biological replicates. **C.** Same as

715 (B). The experiment shown is representative of two independently performed

716 biological replicates. **D.** Same as (B) except that lambda phosphatase (2ul) was

717 optionally added, as indicated. Phosphatase was added after the IVTT reactions

718 were finished and prior to addition of the GST proteins. The experiment shown is

719 representative of two independently performed biological replicates.

720

721 **Figure 3. NBS1 independently binds to both BRCT1 and BRCT2 from TOPBP1.**

722 **A-C.** Bugs-Bunny binding assays, using the indicated proteins, were performed

723 exactly as in Figure 2B. The experiments shown are representative of two

724 independently performed biological replicates. **D-E.** Cartoons highlighted the

725 different ways that RAD9Tail and NBS1 interact with TOPBP1's BRCT0-2 region. See

726 text for details.

727

728 **Figure 4. NBS1 uses its BRCT1 to bind directly to the TOPBP1 BRCT0-2 region.**

729 **A.** Cartoons summarizing the domains located within the N-terminus of NBS1 and

730 the various truncations used in the binding assays. **B-E.** Bugs-Bunny binding assays,

731 using the indicated proteins, were performed exactly as in Figure 2B with exception

732 that MBP and not GST fusion proteins were utilized. The experiments shown are

733 representative of two independently performed biological replicates. **F.** As detailed

734 in the Methods section, the indicated purified, recombinant proteins were mixed

735 and then assessed for interaction by MBP pull-down. The experiment shown is

736 representative of two independently performed biological replicates.

737

738 **Figure 5. Delineation of the NBS1 binding region within TOPBP1's BRCT1**

739 **domain.**

740 **A.** Cartoons summarizing the various truncations used in the binding assays. These

741 MBP-fusion proteins were produced by IVTT and used in Bugs-Bunny binding

742 assays with recombinant GST-NBS1 1-400. **B-E.** Bugs-Bunny binding assays, using

743 the indicated proteins, were performed exactly as in Figure 2B. The MBP fusions

744 were detected with an antibody recognizing the MBP tag. The experiments shown

745 are representative of two independently performed biological replicates. **F.** The

746 sequence of TOPBP1's BRCT1 domain is shown. The red box highlights the

747 experimentally defined NBS1 binding region 1.

748

749 **Figure 6. Delineation of the NBS1 binding region within TOPBP1's BRCT2**

750 **domain.**

751 **A.** Cartoons summarizing the various truncations used in the binding assays. These
752 MBP-fusion proteins were produced by IVTT and used in Bugs-Bunny binding
753 assays with recombinant GST-NBS1 1-400. **B-D.** Bugs-Bunny binding assays, using
754 the indicated proteins, were performed exactly as in Figure 2B. The MBP fusions
755 were detected with an antibody recognizing the MBP tag. The experiments shown
756 are representative of two independently performed biological replicates. **E.** The
757 sequence of TOPBP1's BRCT2 domain is shown. The red box highlights the
758 experimentally defined NBS1 binding region 2. **F.** Cartoon showing the alanine
759 scanning mutants used to define the critical amino acids within NBR2 that are
760 needed to bind NBS1. **G-H.** Bugs-Bunny binding assays, using the indicated proteins,
761 were performed exactly as in Figure 2B. The experiments shown are representative
762 of two independently performed biological replicates.
763
764 **Figure 7. TOPBP1's BRCT1 and BRCT2 use similar sequences to bind TOPBP1's**
765 **BRCT4&5 domains as for NBS1.**
766 **A-B.** Bugs-Bunny binding assays, using the indicated proteins, were performed
767 exactly as in Figure 2B. The MBP constructs are the same as those depicted in
768 Figures 5A and 6A. The experiments shown are representative of two independently
769 performed biological replicates. **C.** The sequences for NBR1 and NBR2 are shown
770 and the relevant regions for binding to BRCT4&5 are shown.
771
772 **Figure 8. A comparison of the TOPBP1::NBS1 interactions to previously**
773 **studied BRCT::BRCT interactions involving XRCC1, DNA ligase II, and ECT2.**

774 **A.** The sequences for TOPBP1's BRCT1 and BRCT2 domains are shown. The
775 canonical BRCT domain secondary structures are also highlighted. Shown in red
776 lettering are NBR1 and NBR2. **B.** The tertiary structure of human TOPBP1's BRCT0-
777 2 region is shown at two different angles. The regions corresponding to NBR1 and
778 NBR2 are indicated and colored in beige. The images were generated using NCBI's
779 web-based "Structure" protein analysis tool. **C.** The sequence of XRCC1's BRCT1
780 domain is shown and the canonical BRCT domain secondary structures are
781 highlighted. Shown in red lettering are amino acids that mediate the interaction
782 with DNA ligase III. **D.** The BRCT1 domains from TOPBP1 and ECT2 are aligned.
783 Shown in red lettering are the ECT2 amino acids that mediate the interaction with
784 phosphorylated CYK4. **E.** The sequence of *Xenopus* TOPBP1's NBR2 region is shown
785 and compared to its human and *Drosophila* counterparts. Shown in red lettering are
786 conserved amino acids for the human and fly proteins.
787

788 **Figure 1**

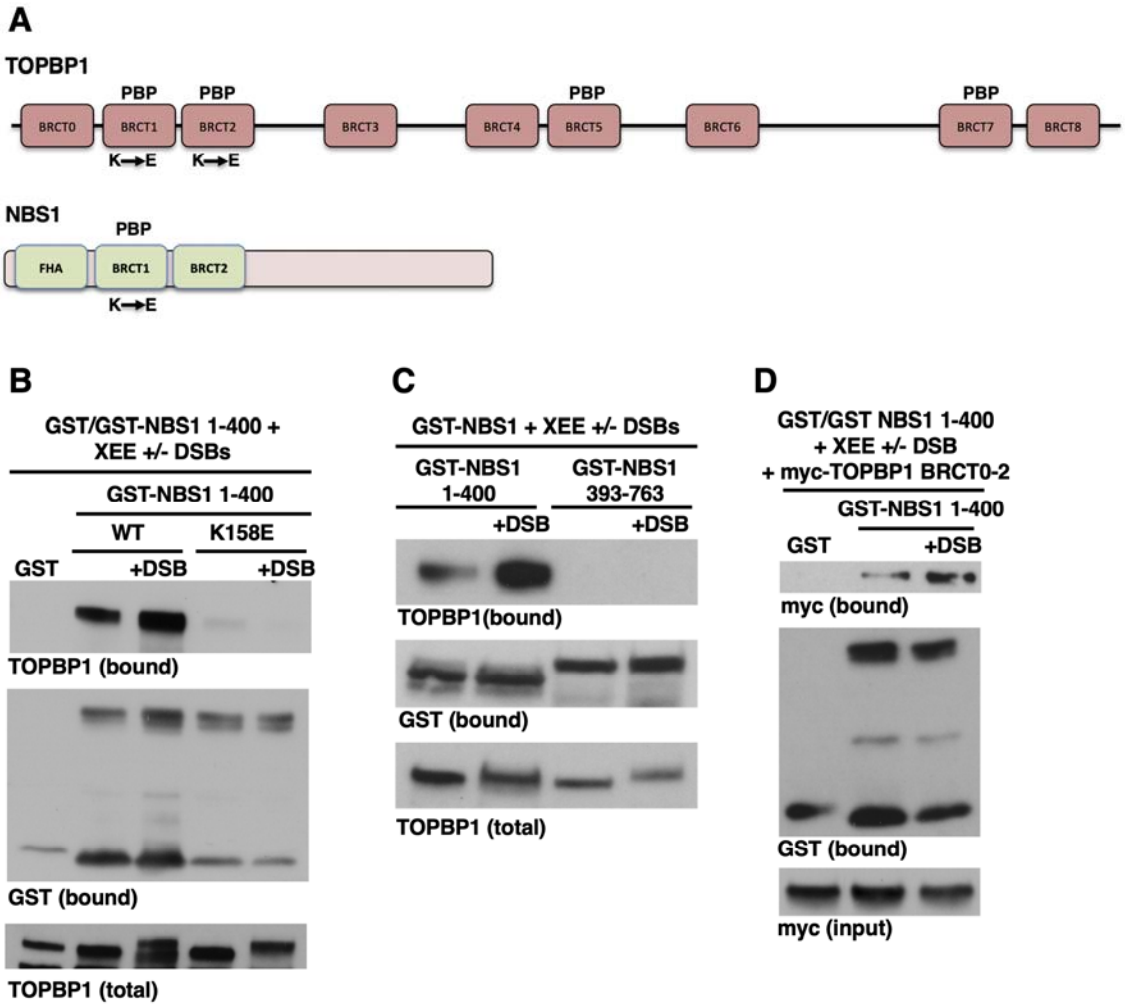

789

790

791 **Figure 2**

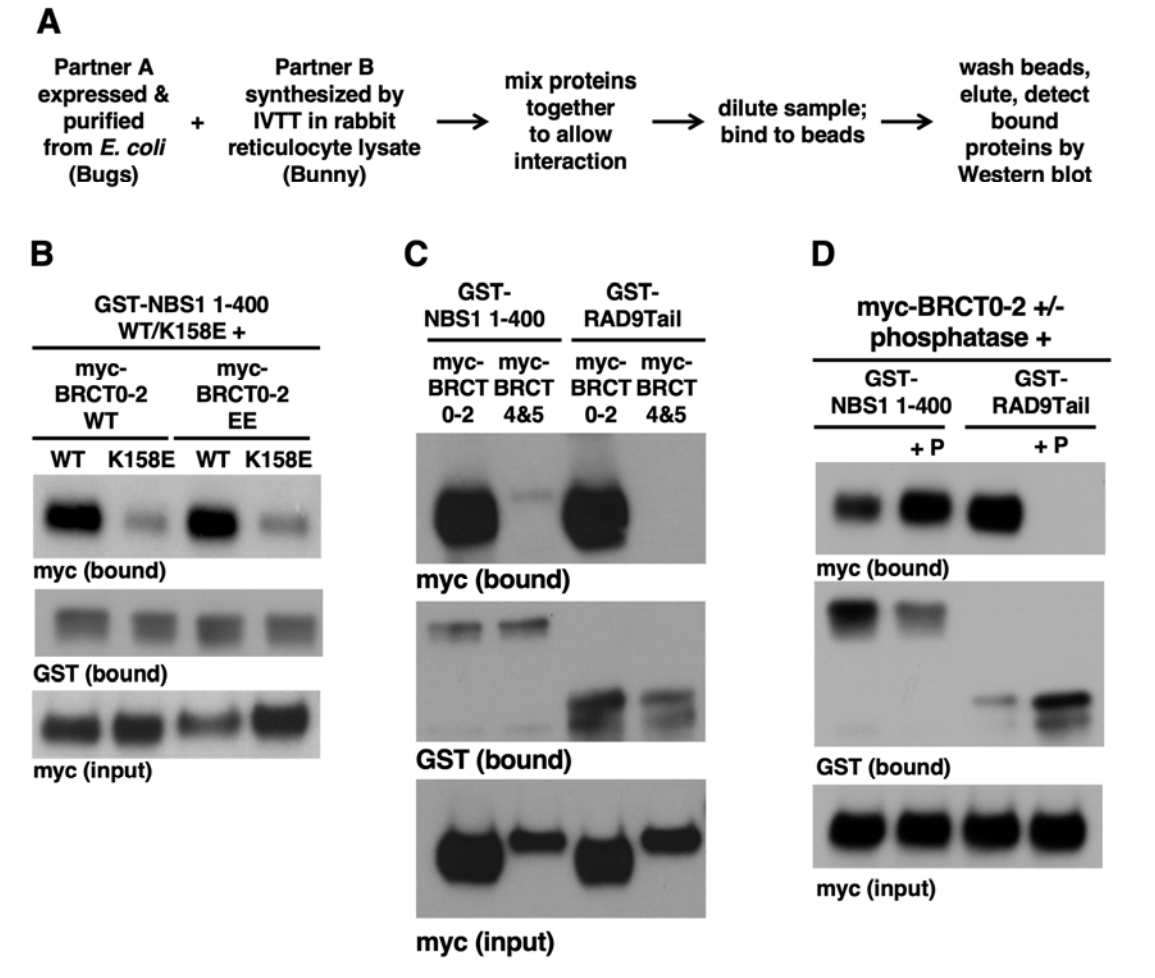

792

793

794 **Figure 3**

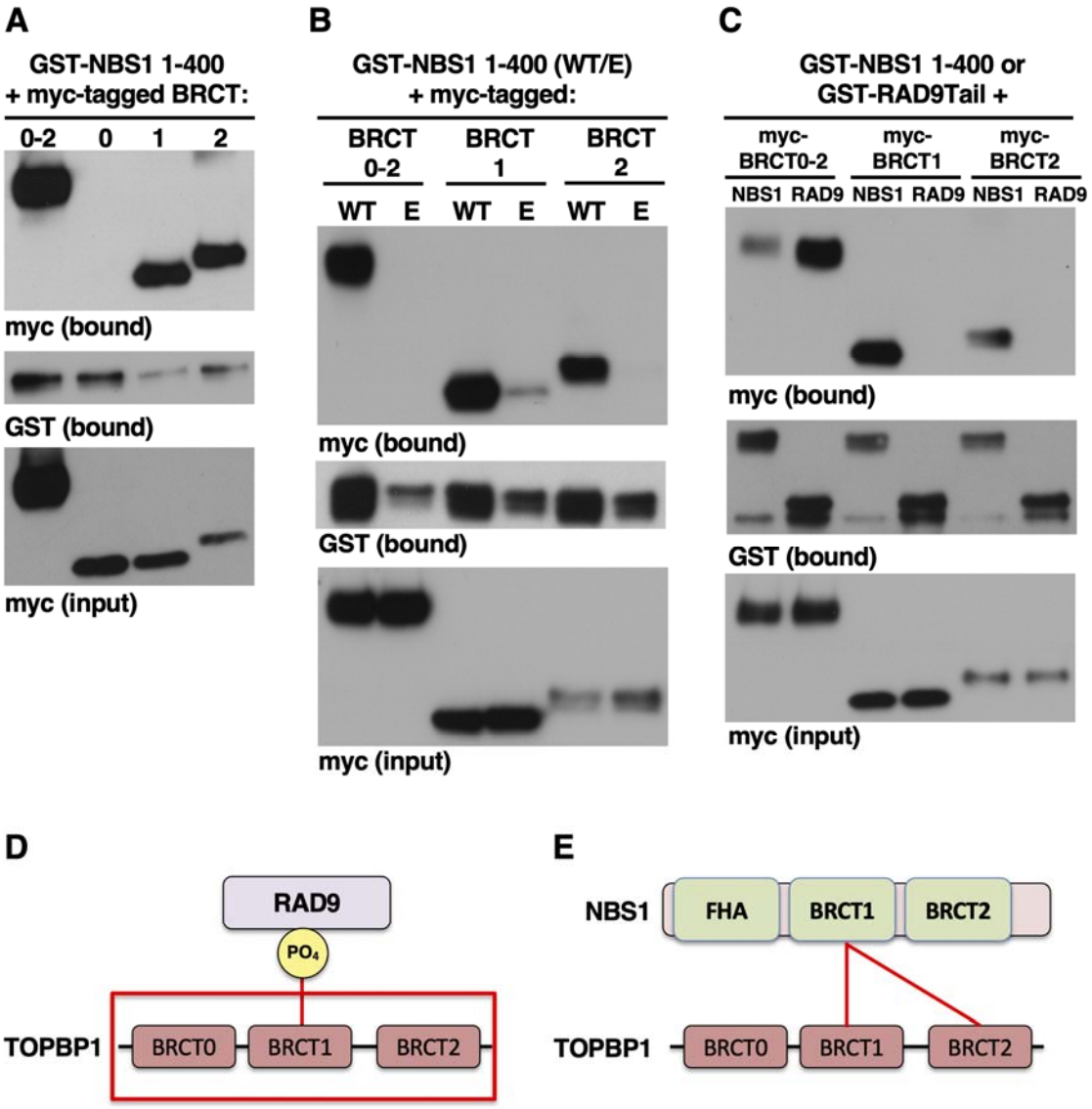

795

796

797 **Figure 4**

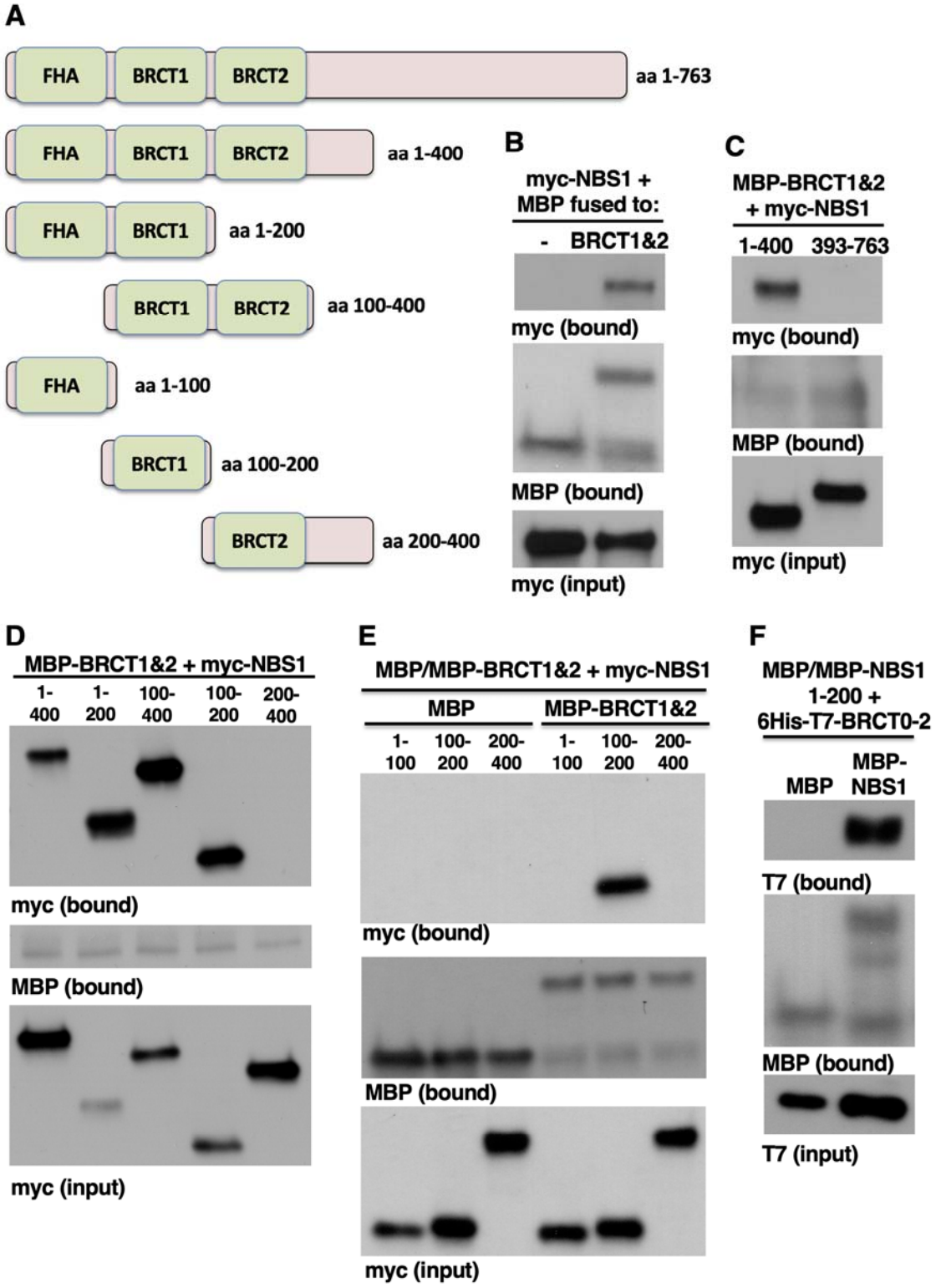

798

799

800 **Figure 5**

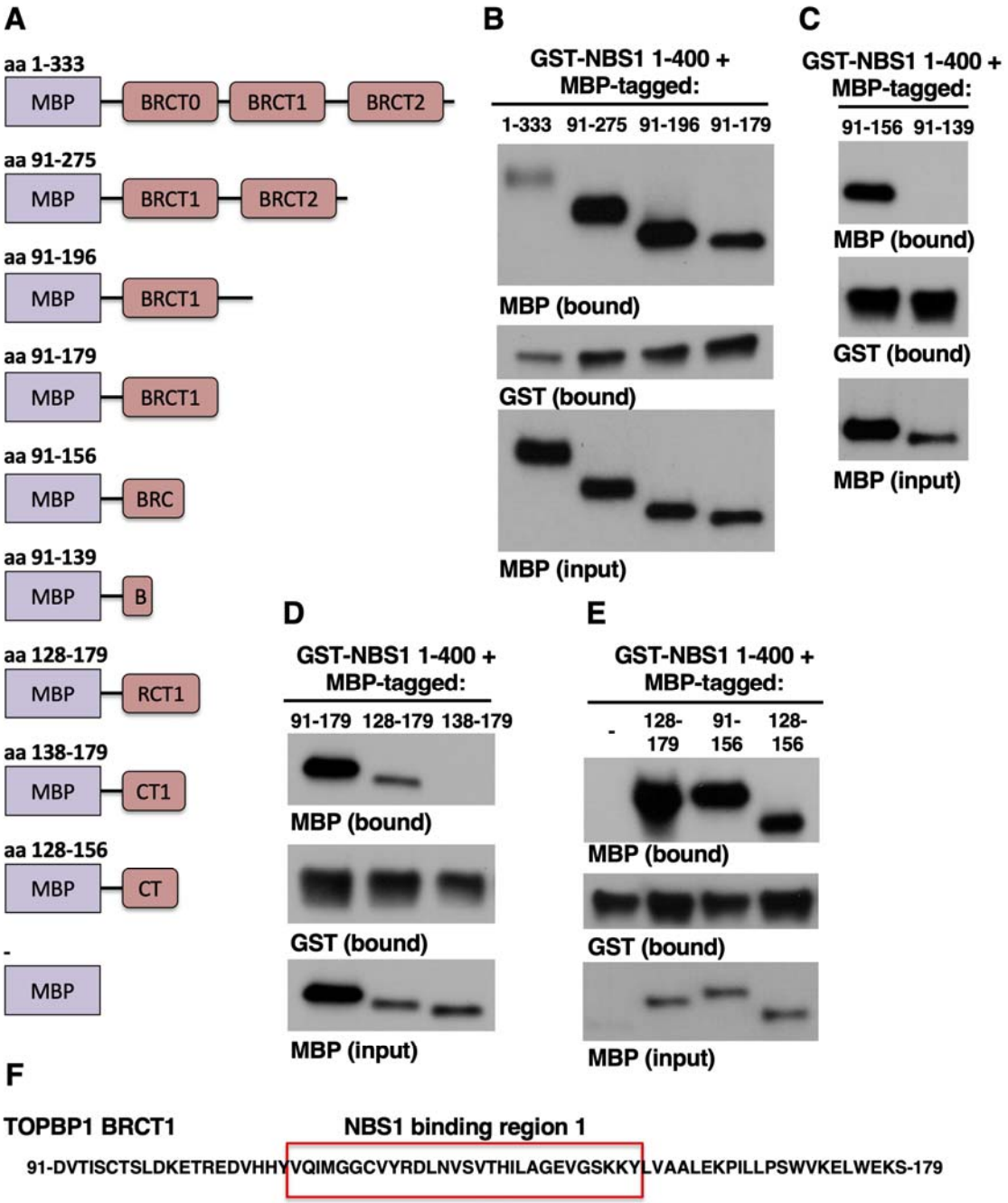

801

802

803 **Figure 6**

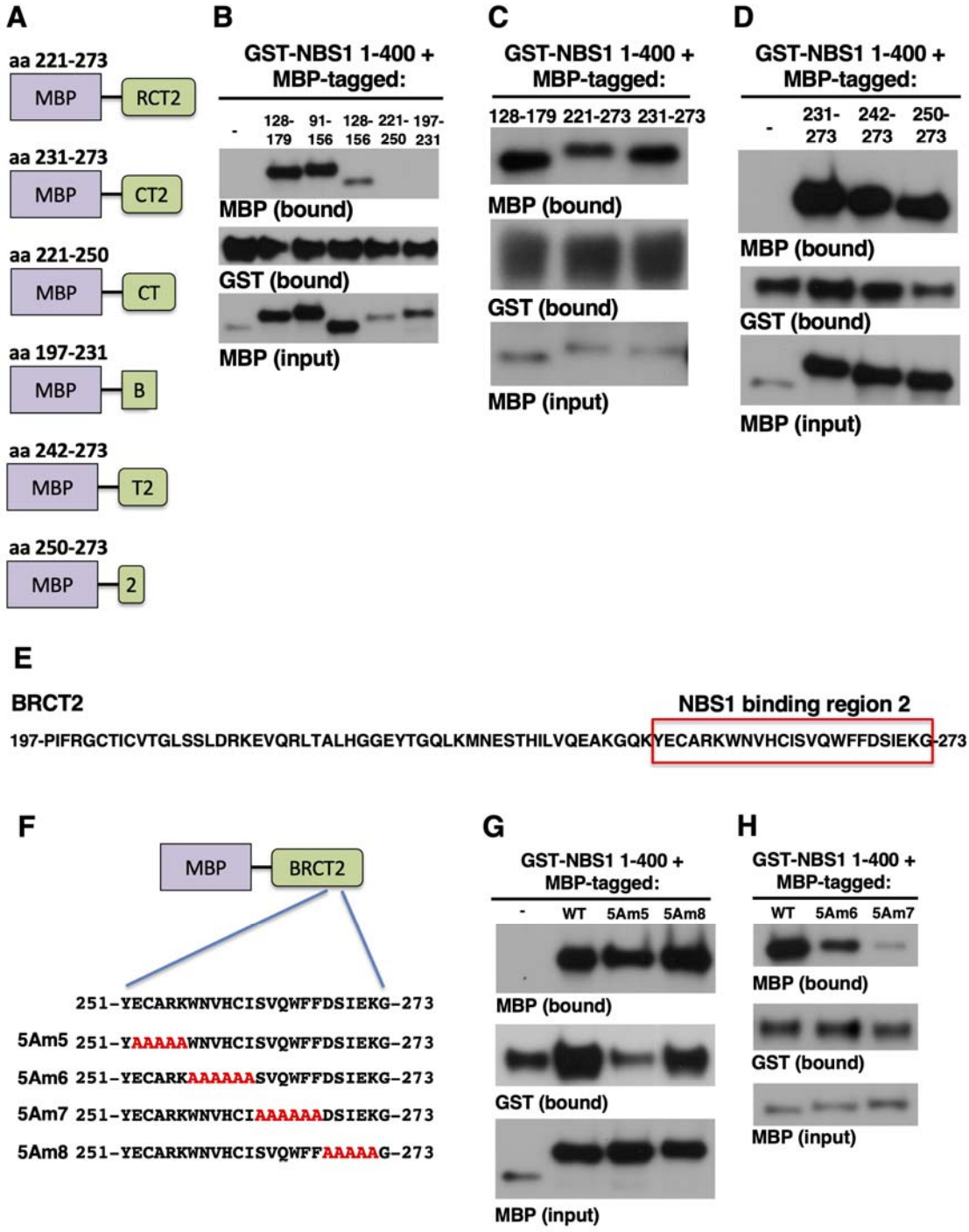

804

805

806 **Figure 7**

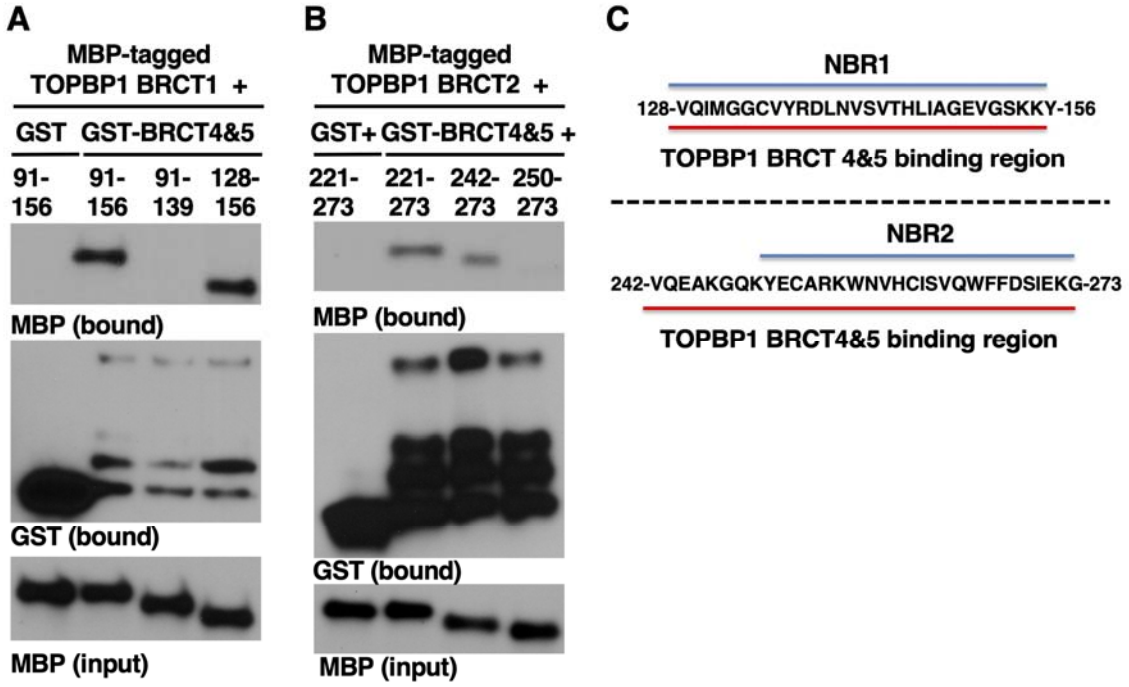

807

808

809 **Figure 8**

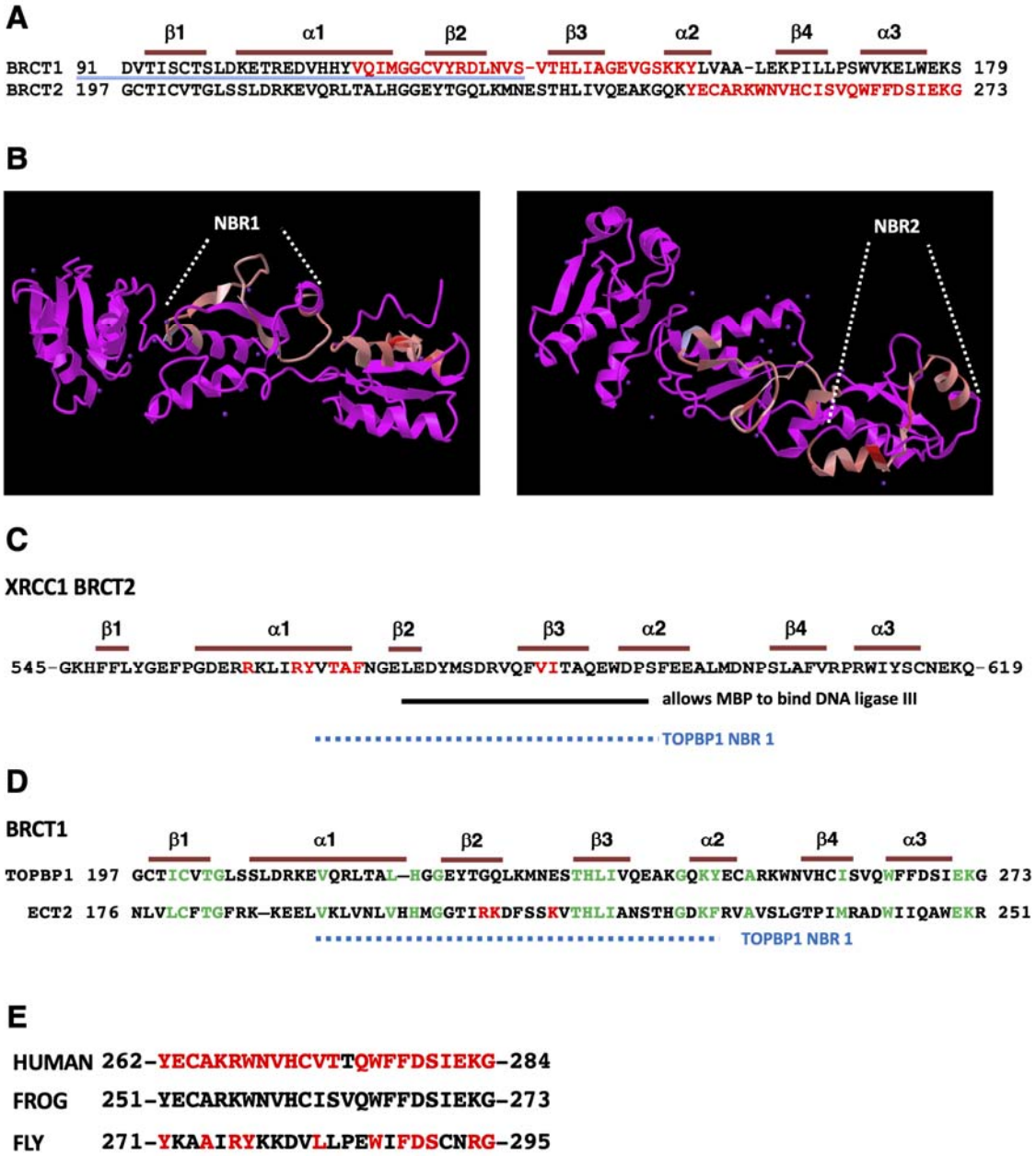

810